Scanning Microscopy Vol. 12, No. 1, 1998 (Pages 131-138) 0891-7035/98$5.00+.25
Scanning Microscopy International, Chicago (AMF O'Hare), IL 60666 USA

BACKSCATTERING OF POSITRONS FROM SOLID TARGETS

Maurizio Dapor*, and Antonio Miotello[1]

Centro Materiali e Biofisica Medica, Istituto Trentino di Cultura, I 38050 Povo, Trento, Italy
[1]Istituto Nazionale per la Fisica della Materia and Dipt. Fisica, Univ. Trento, I 38050 Povo, Trento, Italy

(Received for publication March 11, 1996 and in revised form September 7, 1996)

Abstract

As recently shown by Vicariek and Urbassek, the mean number ν of the large angle collisions suffered by a charged particle before slowing down to rest in a solid is a quantity that plays an important role in determining the backscattering probability from solid targets. ν depends both on the range and on the transport cross-section of the particles penetrating the solid. In this paper, we describe a computational method for calculating ν for low energy positrons (particle kinetic energy, $E_0 < 5$ keV). This method is based on a numerical code for the calculation of the differential elastic scattering cross section and on the stopping power calculation of Ashley. Then, we compare the backscattering coefficients, obtained by using the calculated values of ν, to the results obtained with Monte Carlo simulations and to the available experimental data.

Key Words: Elastic scattering cross section, stopping power, transport cross section, range, large angle collisions, Monte Carlo simulations, backscattering coefficient, low energy positrons.

* Contact for correspondence: Maurizio Dapor, address as above.

Telephone number: 39 461 314479
FAX number: 39 461 810851
E.Mail: dapor@cmbm.itc.it

Introduction

Due to the increasing interest in material analysis techniques, such as electron probe microanalysis, electron-energy-loss-spectroscopy, Auger electron spectroscopy, positron annihilation spectroscopy etc., the theoretical study of the effects of the irradiation of solid targets by charged particles has recently received great attention [1, 2, 3, 4, 6, 8, 9, 10, 11, 12, 13, 14, 15, 16, 17, 18, 19, 20, 22, 23, 24, 25, 26, 27, 28, 30, 31, 33, 34, 35, 36].

In this paper, we study monoenergetic beams of positrons striking solid targets: thus, it is worth to summarize some general aspects of the problem of the interaction of charged particles with solid targets.

When a particle beam impinges on a solid target, some particles, after a number of elastic and inelastic collisions with the atoms of the target, come back and emerge from the surface, while other particles are transmitted and emerge from the back of the sample. The remaining particles are trapped into the target. The fractions of trapped, backscattered and transmitted particles depend on the thickness of the target. For bulk targets, the fraction of backscattered particles reaches its saturation value, generally called the backscattering coefficient. The backscattering coefficient depends on the type of particles, on their primary energy, on the target mean atomic number, and on the incidence angle. In this paper, we consider low energy positrons and we study the dependence of the backscattering coefficient on the target mean atomic number, positron incidence angle, and primary energy. We compare our results to the available experimental data and to the results of Monte Carlo simulations.

As recently shown by Vukanic *et al.* [36] and by Vicanek and Urbassek [35], the backscattering coefficient is strongly related to the mean number ν of large angle collisions suffered by the particle before slowing down to rest. ν depends on the type of particles, on their primary energy, and on the target mean atomic number: it is, indeed, a function of the elastic and inelastic processes suffered by the particles travelling in the solid target. Thus, the calculation of ν, requires a very accurate knowledge of the elastic and inelastic scattering processes.

Symbol Table

E_0	primary particle kinetic energy [eV]
E	particle kinetic energy [eV]
α	incidence angle relative to the surface normal [rad]
θ	scattering angle [rad]
$d\sigma/d\Omega$	differential elastic scattering cross section [$Å^2$/ster]
σ_{tot}	total elastic scattering cross section [$Å^2$]
σ_{tr}	transport elastic scattering cross section [A^2]
dE/ds	stopping power [ev/Å]
R	range [Å]
η	backscattering coefficient
N	number of atoms per unit of volume in the target [$Å^{-3}$]
ν	mean number of the large angle collisions suffered by the particle before slowing down to rest

In a collision event with an atomic electron or a nucleus, the incident positron loses energy and changes direction. Atomic electron excitations or ejections and plasmon excitations affect the energy dissipation of the incident positron and only slightly its direction in the solid, while nuclear collisions are nearly elastic and deflect the incident positron without relevant energy transfer, due to the large mass difference between the incident particle and the nucleus. Actually, a positron can lose a large fraction of its energy in a single collision (or even be annihilated). Nevertheless the so called continuous slowing down approximation is generally accepted: in such an approximation, the positron is assumed to continuously dissipate its energy during its travel inside the solid. In this approach, the relevant function to describe inelastic events is the so called stopping power, namely the mean energy loss per unit path length in the solid target. In the present work, we used the Ashley [2] stopping power, which is very accurate and allows us to study the behaviour of low energy electrons and positrons (particle kinetic energy, E < 10 keV).

The other important function needed to describe the beam behaviour inside the solid is the differential elastic scattering cross section. Unfortunately, for low energy positrons, no analytical expressions exist to compute elastic scattering processes and rather time consuming numerical approaches are necessary. The numerical calculation of differential, total and transport elastic scattering cross sections were obtained, for the atomic numbers higher than 18, by using the very accurate atomic potential recently given by Salvat *et al.* [32]. The light elements have been described by the Cox and Bonham potential [7]. The results are in very good agreement with the experimental ones [17] due to the following possible reasons: (a) the use of the Dirac equation instead of the Schrödinger one for the phase shifts computation; (b) the very accurate atomic potential used; and (c) the introduction of solid state effects in the atomic potential.

Once the elastic and inelastic processes are known with good accuracy, then ν can be calculated. The backscattering coefficient η is proportional to ν, when $\nu < 1$ [35, 36], being, in general a simple function of ν [35]. It is also worth pointing out that, in the energy range examined, we found that ν, is always smaller for positrons than for electrons. It seems then reasonable to conclude that electrons have a probability of backscattering larger than positrons, in agreement with the experimental work of Baker and Coleman [4] and Massoumi *et al.* [23, 24].

In order to simplify the computation of ν, in this paper, we propose an analytical expression obtained through the best fit of the computed numerical results. The backscattering coefficient calculated by introducing the proposed equation in the Vicanek and Urbassek theory [35] is then compared to the Coleman *et al.* [6] experimental data. Afterwards, based on the same elastic and inelastic processes modelling, a Monte Carlo simulation is proposed and results concerning backscattering processes are compared to Monte Carlo data found in the recent literature. The comparisons allow us to conclude that the agreement between theory and experiment, for angles of incidence relative to the surface normal lower than ~ 60°, is better by using the Vicanek and Urbassek theory than the Monte Carlo modelling. On the other hand, for angles of incidence higher than 60°, Monte Carlo simulated data are in very good agreement with the experiment.

Theoretical Framework

The mean number of large angle collisions

If σ_{tr} is the positron transport cross section and R the positron range of penetration, defined by

$$R = \int_{E_0}^{0} \frac{dE}{dE/ds} \tag{1}$$

where dE/ds is the energy lost per unit of length and E_0 is the primary energy, then the mean number of large angle collisions is defined as

$$\nu = NR\sigma_{tr} \tag{2}$$

where N is the number of atoms per unit of volume in the solid target.

The computation of the range was performed by Gaussian quadrature of the polynomial best fits of the stopping power numerical results given by Ashley [2]. The

integration was performed from the primary energy E_0 to 100 eV instead of 0 eV. For the elastic scattering cross sections computation, we have followed the scheme of Lin *et al.* [21] and Bunyan and Schonfelder [5]. The Dirac equation was reduced to the following first order differential equation:

$$\frac{d\phi_l^{\pm}(r)}{dr} = \frac{k^{\pm}}{r}\sin[2\phi_l^{\pm}(r)] - \cos[2\phi_l^{\pm}(r)] + W - V(r) \tag{3}$$

where the function $\phi_1^{\pm}$(r) is related to the phase shifts, W is the total energy, r the distance between the colliding particle and the nucleus and V(r) is the atomic potential energy that we will briefly discuss below. Energies are expressed in units of mc^2 and the lengths r are expressed in $h/2\pi mc$ (m = electron mass, c = speed of light, h = Planck's constant). ± symbols denote the spin up and the spin down cases: in particular $k^+ = -l-1$ (and $j = l + 1/2$) while $k^- = l$ (and $j = l-1/2$).

For each quantum number *l*, the two phase shifts $\delta_l^{\pm}$ can be obtained by using the following equation:

$$\tan\delta_l^{+} = \frac{Kj_{l+1}(Kr) - j_l(Kr)[(W+1)\tan\phi_l^{\pm} + (1+l+k^{\pm})/r]}{Kn_{l+1}(Kr) - n_l(Kr)[(W+1)\tan\phi_l^{\pm} + (1+l+k^{\pm})/r]} \tag{4}$$

where $K^2 = W^2-1$, j_l and n_l are respectively the regular and the irregular spherical Bessel functions and $\phi_1^{\pm}$ is the limit of $\phi_1^{\pm}$(r) for $r \to \infty$.

The atomic potential was that of Hartree-Fock for atomic numbers lower than 19 and that of Dirac-Hartree-Fock-Slater for atomic numbers higher than 18. We used the best fit functions proposed by Cox and Bonham [7] for the Hartree-Fock potential and by Salvat *et al.* [32] for the Dirac-Hartree-Fock-Slater potential.

Solid state effects should be introduced when the target atom is bound in a solid. Indeed, when the target atom is bound in a solid, the outer orbitals of the atom are modified. In order to consider such alterations solid state effects have been introduced by using the muffin-tin model in which the potential of each atom of the solid is altered by the nearest neighbour. Let us introduce the radius of the Wigner-Seitz sphere:

$$rWS = 0.7346(A/\rho)^{1/3}\ \text{Å} \tag{5}$$

where A is the atomic weight and ρ the mass density (g/cm^3).

Assuming that the nearest neighbour is located at a distance of $2r_{WS}$, the resulting potential is given by:

$$\begin{aligned} V_{solid}(r) &= V(r) + V(2r_{WS} - r) - 2V(r_{WS}), && r < r_{WS};\\ V_{solid}(r) &= 0, && r \geq r_{WS}. \end{aligned} \tag{6}$$

The term $2V(r_{WS})$, introduced in order to shift the energy scale so that $V_{solid}(r \geq r_{WS}) = 0$, has been also subtracted from the kinetic energy of the incident particle. This approach in describing elastic scattering in solids has been adopted, for example, by Czyzewski *et al.* [81 and by Salvat and Mayol [33].

The values of $\phi_1^{\pm}$ have been computed by numerical integration of the Dirac equation (3) by using a fourth order Runge-Kutta method. Afterwards they have been used for calculating the phase shifts by the equation (4).

Once the values of the phase shifts are known, the differential elastic scattering cross section can be calculated as [29]

$$\frac{d\sigma}{d\Omega} = |f|^2 + |g|^2 \tag{7}$$

where the scattering amplitudes f and g are given by

$$f(\theta) = \frac{1}{2iK}\sum_{l=0}^{\infty}\{(l+1)[\exp(2i\delta_l^-) - 1] + l[\exp(2i\delta_l^+) - 1]\}P_l(\cos\theta) \tag{8}$$

$$g(\theta) = \frac{1}{2iK}\sum_{l=1}^{\infty}[-\exp(2i\delta_l^-) + \exp(2i\delta_l^+)]P_l^1(\cos\theta) \tag{9}$$

In these equations P_1 represent the Legendre polynomials and

$$P_l^1(x) = (1-x^2)^{1/2}\frac{dP_l(x)}{dx} \tag{10}$$

The computation of the total and transport elastic scattering cross sections defined, respectively, as

$$\sigma_{tot} = 2\pi\int_0^{\pi}\frac{d\sigma}{d\Omega}\sin\theta d\theta \tag{11}$$

$$\sigma_{tr} = 2\pi\int_0^{\pi}(1-\cos\theta)\frac{d\sigma}{d\Omega}\sin\theta d\theta \tag{12}$$

has been performed by applying the Bode's rule to the numerically calculated differential cross sections.

Once the transport cross section and the range are known, one can calculate the mean number of large angle collisions.

Our numerical results, which are very accurate for positrons of energy in the range 500 eV < E < 5000 eV [14, 15, 16, 17], may be accommodated in the analytical function:

$$\nu = \exp(\xi_0 + \xi_1 \ln E + \xi_2 \ln^2 E) \quad (13)$$

Here $\xi_i = \xi_i(Z)$, i = 0, 1, 2 and Z is the atomic number of the target. Table 1 gives the values of ξ_i for Al, Cu, Ag and Au (E in eV). The values ξ_i for the whole range of Z will be given in a later publication.

In order to give an idea of the accuracy of the best fit we have presented, in Figure 1, a comparison between eq. (13) and the numerically computed values of ν for positrons in Cu.

The value of the backscattering coefficient can thus be obtained by introducing this expression in the Vicanek and Urbassek formula given by [35]:

$$\eta = (1 + a_1 \frac{\mu_0}{\upsilon^{1/2}} + a_2 \frac{\mu_0^2}{\upsilon} + a_3 \frac{\mu_0^3}{\upsilon^{3/2}} + a_4 \frac{\mu_0^3}{\upsilon^2})^{-1/2} \quad (14)$$

where μ_0 is the cosine of the angle of incidence, $a_1 = 6/\sqrt{\pi}$, $a_2 = 27/\pi$, $a_3 = 27(4/\pi - 1)/\sqrt{\pi}$ and $a_4 = (3/2 - \sqrt{2})^{-2}$.

The Monte Carlo simulation

The backscattering coefficient can be computed, of course, also by using a Monte Carlo simulation [1, 4, 6, 11, 13, 19, 23, 24, 31]. Here we describe the Monte Carlo simulation we used for the backscattering coefficient computation for positrons of primary energies in the range 500 eV < E_0 < 5000 eV. The Monte Carlo scheme is essentially the same as in Reference [11], but the inelastic and the elastic processes were described by the equations presented in the previous subsection.

The stopping power used in the present work was that reported by Ashley [2].

The path length distribution is assumed to follow a Poisson type law. As a consequence, the step length Δs is given by

$$\Delta s = \lambda_{tot} \ln(r_1) \quad (15)$$

where

$$\lambda_{tot} = (1/N\sigma_{tot}) \quad (16)$$

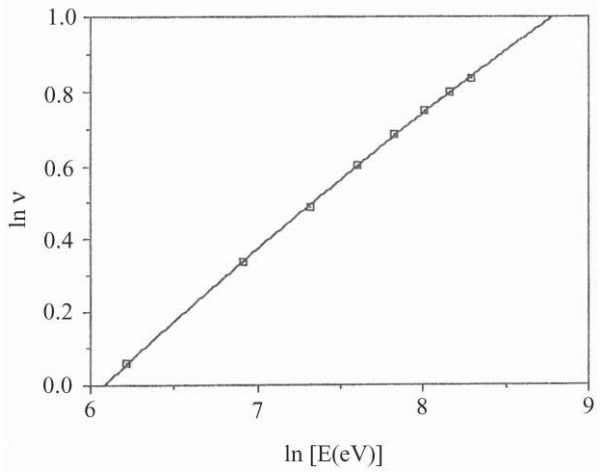

Figure 1. Positrons in Cu: comparison between Equation 13 (solid) and the numerically computed values of ν (squares). Energies are in eV.

Table 1. The values of ξ_i (Eq. 13) relative to Al, Cu, Ag and Au (E in eV).

Z	ξ0	ξ1	ξ2
13	-4.4277	1.0119	-0.0526
29	-3.374	0.6825	-0.021
47	-6.3427	1.3846	-0.0628
79	-5.6038	1.146	-0.0413

and r_1 is a random number uniformly distributed in the range 0-1.

The energy loss ΔE along the trajectory Δs is approximated by

$$\Delta E = (dE/ds)\, \Delta s \quad (17)$$

Concerning the interpolation methods used to sample the scattering angle, we fitted the differential elastic scattering cross section by using the following function:

$$(d\sigma/d\Omega) = \{a / (1 - \cos\theta)^b\} \quad (18)$$

The values of *a* and *b* were obtained by looking for the best fit of the numerically calculated values of the differential elastic scattering cross section.

The polar scattering angle θ after an elastic collision, is calculated by assuming that the probability

Table 2. Backscattering coefficients of 3 keV positrons for normal incidence: present analytical and Monte Carlo calculations are compared to experimental data and to other authors Monte Carlo calculations. Aers' data: Best fit of Aers' Monte Carlo data.

Z	Coleman et al Monte Carlo data (1992)	Aers Monte Carlo data (1994)	Ghosh and Aers Monte Carlo data (1995)	Present Monte Carlo data	Present eqs. (13) and (14)	Coleman et al Experimental data (1992)
13	0.115	0.115	0.123	0.114	0.107	0.086
29	0.194	0.188	0.138	0.191	0.159	0.177
47	0.182	0.175	0.227	0.192	0.156	0.168
79	0.242	0.232	0.239	0.245	0.186	0.186

$$P(\theta) = \frac{2\pi \sum_{\theta_{min}}^{\theta} \frac{d\sigma}{d\Omega} \sin\vartheta d\vartheta}{\sigma_{tot}} \qquad (19)$$

of elastic scattering into an angular range between θ_{min}. and θ is a random number r_2 uniformly distributed in the range 0-1. In order to avoid divergence, the integration was performed from $\theta = \theta_{min} > 0$. By assuming $\theta_{min} = 5°$, the error in evaluating σ_{tr} for copper was 2 % while for gold it was less than 1 %. Errors of ~ 10 % were obtained in the evaluation of σ_{tot}.

Equations (18) and (19) allow us to obtain the values of $\cos\theta$ for any random number $P(\theta) = r_2$ by the following closed formula:

$$\mathbf{cos}\theta = 1 - [(2^{1-b} - h)P(\theta) + h]^{1/(1-b)} \qquad (20)$$

where

$$h = (1 - \mathbf{cos}\theta_{min})^{1-b} \qquad (21)$$

The azimuthal angle ψ can take on any value in the range 0-2π selected by a random number r_3 uniformly distributed in that range.

Both the θ and the ψ angles are calculated relative to the last direction in which the particle was moving before the impact. The direction θ_z' in which the particle is moving after the last deflection, as related to the z direction, is given by

$$\cos\theta_z' = \cos\theta_z \cos\theta + \sin\theta_z \sin\theta \cos\psi \qquad (22)$$

where θ_z is the angle relative to the z direction before the impact.

The step motion Δz along the z direction is then calculated by

$$\Delta z = \Delta s \cos\theta_Z' \qquad (23)$$

The new angle θ_Z' then becomes the incident angle θ_Z for the next path length.

The adopted absorption energy, i.e., the energy at which positrons are assumed to effectively stop in the medium, was 100 eV.

Results and Discussion

In Table 2, the backscattering coefficient for normal incidence of 3 keV positrons is reported, for various pure elements, as calculated by introducing eq. (13) in the Vicanek and Urbassek theory [35] and also by using the present Monte Carlo simulation. For a comparison, the experimental data of Coleman *et al.* [6] and the Monte Carlo data of various authors [1, 6, 19] have been reported.

The comparisons allow us to conclude that the agreement between theory and experiment is slightly better by using the Vicanek and Urbassek expression than the Monte Carlo modelling. Monte Carlo simulations seem to give results systematically higher than the experiment (withjust an exception). We believe that the reason of this slight discrepancy between Monte Carlo data and experimental data is in the approximations involved in the interpolation of the differential elastic scattering cross section necessary for the computation of the scattering angle at every step of each trajectory. Another possibility is that the surface contaminations of the targets have an influence in lowering the experimental backscattering coefficient: since, however, cleaning by ion sputtering *in situ* were performed, it seems that the influence of

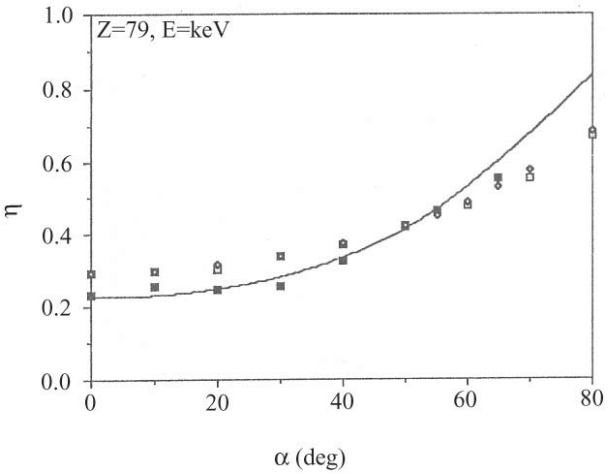

Figure 2. Angular dependence of the backscattering coefficient for 5 keV positrons impinging on Au as computed by using the Equation 13 and the Vicartek and Urbassek theory (solid line) compared to the present Monte Carlo simulation (diamonds), the Monte Carlo data of Coleman *et al*. [6] (empty squares) and the experimental data of Coleman et al. [6] (filled squares).

contamination on the experimental data, if any, should be negligible.

In order to study the influence of the angle of incidence relative to the surface normal, α, we reported, in Figure 2, the angular dependence of the backscattering coefficient concerning 5 keV positrons impinging on gold as computed by using the Vicanek and Urbassek theory [35] and the present Monte Carlo simulation. The Monte Carlo data of Coleman et al. [6] and the experimental data of Coleman et al. [6] were also reported for a comparison.

This comparison confirms the good agreement between the analytical model and the experimental data for angles of incidence, relative to the surface normal, lower than ~ 60°. For very high angle of incidence, on the other hand, the Monte Carlo approaches give better results.

We can then conclude that, at least for low angles of incidence and energies < 5 keV, the formula proposed by Vicanek and Urbassek gives results in good agreement both with experimental data and Monte Carlo theoretical results. A comparison with experimental data obtained in other laboratories is necessary to better understand the reasons of the slight discrepancy between Vicanek and Urbassek's theory and Monte Carlo simulations.

Conclusion

We have proposed an analytical expression for the mean number ν of the positrons large angle collisions in solid targets obtained through a best fit of our computed numerical results. The backscattering coefficient calculated by introducing the proposed equation in the Vicanek and Urbassek theory was then compared to the Coleman *et al*. [6] experimental data. Afterwards, based on the same elastic and inelastic modelling, a Monte Carlo simulation was proposed and its results concerning backscattering were also compared to experimental and to Monte Carlo data that can be found in the recent literature. The comparisons allow us to conclude that, for positron energies less than 5 keV, the agreement between theory and experiment is very good using both the Vicanek and Urbassek theory and the Monte Carlo simulation.

References

[1] Aers GC (1994) Positron stopping profiles in multilayered systems. J. Appl. Phys. **76**, 1622-1632.

[2] Ashley JC (1990) Energy loss rate and inelastic mean free path of low energy electrons and positrons in condensed matter. J. Electron Spectrosc. Relat. Phenom. **50**, 323-334.

[3] Asoka Kurnar P, Lynn KG, Welch DO (1994) Characterization of defects in Si and SiO2 Si using positrons. J. Appl. Phys. **76** 4935-4982.

[4] Baker JA, Coleman PG (1988) Measurement of coefficients for the back-scattering of 0.5-30 keV positrons from metallic surfaces. J. Phys. C: Solid State Phys. **21**, L875-L880

[5] Bunyan PJ, Schonfelder JL (1965) Polarization by mercury of 100 to 2000 eV electrons. Proc. Phys. Soc. **85**, 455-462.

[6] Coleman PG, Albrecht L, Jensen KO, Walker AB (1992) Positron backscattering from elemental solids. J. Phys.: Condens. Matter **4** 10311-10322.

[7] Cox Jr. HL, Bonham RA (1967) Elastic electron scattering amplitudes for neutral atoms calculated using the partial wave method at 10, 40, 70, and 100 kV for Z = 1 to Z = 54. J. Chem. Phys. **47**, 2599-2608.

[8] Czyzewski Z, MacCallum DO, Romig A, Joy DC (1990) Calculations of Mott scattering cross section. J. Appl. Phys. **68** 3066-3072.

[9] Dapor M (1991) Penetration of an electron beam in a thin solid film: The influence of backscattering from the substrate. Phys. Rev. B **43**, 10118-10123.

[10] Dapor M (1992) Theory of the interaction between an electron beam and a thin solid film. Surf. Sci. **269/270**, 753-762.

[11] Dapor M (1992) Monte Carlo simulation of backscattered electrons and energy from thick targets and surface films. Phys. Rev. B **46**, 618-625.

[12] Dapor M (1993) Backscattering of electrons from multilayers. Phys. Rev. B **48**, 3003-3008.

[13] Dapor M (1993) Mean energy and depth of penetration of electrons backscattered by solid targets. Appl. Surf. Sci. **70/71**, 327-331.

[14] Dapor M (1995) Elastic scattering of electrons and positrons by atoms: Differential and transport cross section calculations. Nucl. Instrum. Meth. B **95**, 470-476.

[15] Dapor M (1995) Analytical transport cross section of medium energy positrons elastically scattered by complex atoms (Z = 1-92). J. Appl. Phys. **77**, 2840-2842.

[16] Dapor M (1995) Penetration of positrons in solid targets. Scanning Microsc. **9**, 939-948.

[17] Dapor M (1996) Elastic scattering calculations for electrons and positrons in solid targets. J. Appl. Phys. **79**, 8406-8411.

[18] Dupasquier A, Zecca A (1985) Atomic and solid-state physics experiments with slow positron beams. La Rivista del Nuovo Cimento 8, 1-73.

[19] Ghosh VJ, Aers GC (1995) Positron stopping in elemental systems: Monte Carlo calculations and scaling properties. Phys. Rev. B **51**, 45-59.

[20] Kawata J, Ohya K (1994) Comparative study of elastic scattering of low-energy electrons, positrons and protons in solids. Nucl. Instrum. Meth. B **90**, 29-31.

[21] Lin SR, Sherman N, Percus JK (1963) Elastic scattering of relativistic electrons by screened atomic nuclei. Nucl. Phys. **45**, 492-504.

[22] Mäkinen J, Palko S, Martikainen J, Hautojärvi P (1992) Positron backscattering probabilities from solid surfaces at 2-30 keV. J. Phys.: Condens. Matter **4**, L503-L508.

[23] Massoumi GR, Hozhabri N, Lennard WN, Schultz PJ (1991) Doubly differential positron-backscattering yield. Phys. Rev. B **44**, 3486-3489.

[24] Massoumi GR, Flozhabri N, Jensen KO, Lennard WN, Lorenzo MS, Schultz PJ, Walker AB (1992) Positron and electron backscattering from solids. Phys. Rev. Lett. **68**, 3873-3876.

[25] Mazzoldi P, Miotello A (1986) Radiation effects in glasses. Rad. Eff. **98**, 39-54.

[26] Miotello A (1984) Mobility and surface recombination processes of primary electrons in dielectric systems during Auger Electron Spectroscopy. Phys. Lett. **103A**, 279-282.

[27] Miotello A, Mazzoldi P (1984) Evidence of an enhanced diffusion process in electron irradiated glasses: A critical analysis of available experimental and theoretical results. J. Phys. C: Solid State Phys. **17**, 3009-3017.

[28] Miotello A, Mazzoldi P (1985) Cooperative transport effects in electron-irradiated glasses Phys. Rev. Lett. **54**, 1675-1678.

[29] Mott NF (1929) The scattering of fast electrons by atomic nuclei. Proc. R. Soc. London, Ser. A **124**, 425-442.

[30] Niedrig H (1982) Electron backscattering from thin films. J. Appl. Phys. **53**, R15-R49.

[31] Nishimura K, Itotani T, Ohya K (1994) Influence of surface roughness on secondary electron emission and electron backscattering from metal surface. Jpn. J. Appl. Phys. **33**, 4727-4734.

[32] Salvat F, Martínez J, Mayol R, Parellada J (1987) Analytical Dirac-Hartree-Fock-Slater screening function for atoms (Z = 1-92). Phys. Rev. A **36**, 467-474.

[33] Salvat F, Mayol R (1993) Elastic scattering of electrons and positrons by atoms. Schrödinger and Dirac partial wave analysis. Computer Phys. Commun. **74**, 358-374.

[34] Schultz PJ, Lynn KG (1988) Interaction of positron beams with surfaces, thin films, and interfaces. Rev. Mod. Phys. **60**, 701-779.

[35] Vicanek M, Urbassek HM (1991) Reflection coefficient of low-energy light ions. Phys. Rev. B **44**, 7234-7242.

[36] Vukanic JV, Janev RK, Heifetz D (1987) Total backscattering of keV light ions from solids at oblique and grazing incidence. Nucl. Instrum. Meth. B **18**, 131-141.

Discussion with Reviewers

K. Ohya: Solid surfaces exhibit a pronounced macroscopic roughness, mostly due to the production process, with a microscopic (atomic scale) roughness superimposed. Our Monte Carlo simulation, which calculates electron backscattering from aluminium with ripple-structured surface bombarded by 1-keV electrons [31], showed a decrease in the backscattering coefficients for normal incidence and a change in their incident angle dependence due to surface roughness. Can you comment on the effect of surface roughness on your results for positron bombardments?

Authors: Surface roughness should influence the backscattering yield, and its dependence on the incident-angle, both for electrons and positrons. In the present work, on the other hand, we did not consider surface roughness: indeed, we are persuaded that surface roughness should substantially influence backscattering if the positron energy is very low. We mean that, at least for the energies we were interested in this paper, it should he reasonable, as a first approximation, to ignore the effects of the surface roughness on the backscattering probability.

K. Ohya: The penetration depth of positrons will be deeper than that of electrons due to smaller cross section for elastic collision of positrons in solids. Therefore, the low-energy component in the energy distribution of backscattered positrons, which is substantially influenced by the surface potential, is expected to be more pronounced than for

electron backscattering. How do you treat the surface potential in your analytical and Monte Carlo calculations?
Authors: The answer is similar to the previous one. We did not take into account the surface potential because, in our opinion, it should become effective only if the positron primary energy is lower than those we have considered.

F. Salvat: As the information feed into the Vicanek and Urbassek analytical formula and into the Monte Carlo calculation is the same, one would expect that both methods yield similar backscattering coefficient, The results in Table 2 and Figure 2 show that this is not the case. Are the differences attributable to any specific approximation introduced in Vicanek and Urbassek's theory?
Authors: Both the Vicanek and Urbassek's theory and the Monte Carlo simulations introduce approximations. Indeed the Vicanek and Urbassek's formula (14) is an empirical expression obtained by interpolating the single collision model ($\nu, << 1$) and the age theory ($\nu >> 1$). Best fits of the elastic scattering and of the stopping power were used, on the other hand, in our Monte Carlo simulation. Thus, we believe that the observed slight differences are attributable to these approximations. Any way, both approaches are in satisfactory agreement with other theoretical calculations and also with the Coleman *et al.* [6] experimental data. The advantage of the analytical approach is, of course, in the simple closed formulas involved: we mean that it is accurate enough for any practical purpose but less computer time consuming than the simulations.

F. Salvat: Energy straggling effects are disregarded in the analytical theory and in your Monte Carlo simulation. Can you comment on how important these effects are for the calculation of the backscattering coefficients?
Authors: The simple approach we adopted, known as the continuous slowing down approximation (CSDA), ignores the statistical fluctuations in both the number of inelastic collisions along a track and the energy loss in each collision. The CSDA is widely used in Monte Carlo simulations and it should be accurate enough for the backscattering coefficient evaluation, at least for practical purposes. Anyway, the introduction of the energy straggling parameter in the description of the inelastic processes should improve the accuracy in the calculation of the backscattering coefficient.

H. Niedrig: How much is the mean number of large angle collisions and hence the backscattering coefficient influenced by the use of the muffin-tin potential for a target atom bound in a solid instead of using the potential for a free atom?
Authors: The mean number of large angle collisions depends on the transport cross section that is not influenced very much by the solid state effects. Let us consider, for example, the case of aluminium. For positrons of 1000 eV, our calculations without solid state effects give a transport cross section of 0.0617 $Å^2$ [14]. If the muffin-tin potential is introduced in the calculation, on the other hand, the transport cross section for the same energy becomes 0.0612 $Å^2$ [17]. Thus, for practical purposes, the calculation of the transport cross section may be performed neglecting the solid state effects and using the analytical formula given in Reference [15].